Probability density functions for advective-reactive transport with uncertain reaction rates

Daniel M. Tartakovsky,[1] Marco Dentz,[2] and Peter C. Lichtner[3]

Received 22 August 2008; revised 14 April 2009; accepted 1 May 2009; published 17 July 2009.

[1] We derive probability density functions for advective transport of a solute that undergoes a heterogeneous chemical reaction involving an aqueous solution reacting with a solid phase. This enables us to quantify uncertainty associated with spatially varying reaction rate constants for both linear and nonlinear kinetic rate laws. While many standard techniques for uncertainty quantification in groundwater hydrology yield only concentration's mean and variance, the proposed approach leads to its full probabilistic description. This allows one to compute so-called rare events (distribution tails), which are required in modern probabilistic risk analyses. We also compute an effective (apparent and upscaled) kinetic rate constant, a parameter that enters transport equations governing the spatiotemporal evolution of mean concentration. We demonstrate that the effective kinetic rate of nonlinear reactions is time-dependent. This behavior provides a possible explanation for the observed discrepancy between laboratory-measured rate constants on uniform grain sizes and measurements in natural systems where the grain size distributions are heterogeneous.

Citation: Tartakovsky, D. M., M. Dentz, and P. C. Lichtner (2009), Probability density functions for advective-reactive transport with uncertain reaction rates, *Water Resour. Res.*, *45*, W07414, doi:10.1029/2008WR007383.

1. Introduction

[2] Quantitative analyses of reactive transport in porous media are notoriously unreliable because of the ubiquitous uncertainty associated with both identification of a proper mathematical model and its reliable parameterization [*Srinivasan et al.*, 2007]. Among the sources of predictive uncertainty in geochemical modeling are the vast dichotomy between the scales on which geochemical parameters are measured (the laboratory scale) and used in numerical simulations (the field scale) [*Lichtner and Tartakovsky*, 2003, and references therein], the sparsity of data and pore structure heterogeneity of porous media. The latter is important even for macroscopically homogeneous formations, since many geochemical reactions are surface-controlled processes that are highly affected by pore geometry, i.e., by heterogeneous distributions of mineral grain sizes. The practical impossibility of identifying pore structures of large volumes of porous media has led to statistical (probabilistic) descriptions of its geometric characteristics, including grain sizes [*Clausnitzer and Hopmans*, 1999; *Tuli et al.*, 2001] and pore sizes [*Lastoskie et al.*, 1993]. This renders transport coefficients (e.g., retardation coefficients and effective kinetic rate constants), which depend on these characteristics, random and the corresponding transport equations stochastic. Solving such equations is equivalent to propagating the parametric uncertainty (which is expressed in terms of probability density functions for the transport coefficients) through a modeling process, thus quantifying the predictive uncertainty in terms of probability density functions for state variables (e.g., concentration and first arrival time).

[3] Much of research in stochastic hydrogeology [e.g., *Rubin*, 2003, and references therein] focused on the first two statistical moments of state variables. The first moment (ensemble mean) is used as an unbiased estimate of a system state, and the second moment (ensemble variance) is used as a measure of uncertainty. These statistical moments can be obtained either indirectly by solving stochastic reactive transport equations with Monte Carlo simulations and other numerical techniques or directly by deriving deterministic equations for each statistical moment [e.g., *Bellin et al.*, 1993]. While providing a measure of predictive uncertainty, such approaches are insufficient for probabilistic risk analyses [e.g., *Tartakovsky*, 2007; *Winter and Tartakovsky*, 2008] that require the knowledge of a state variable's probability density function (pdf).

[4] Monte Carlo simulations and other numerical approaches for solving stochastic reactive transport equations can be used in principle to compute pdf's of system variables. However, three-dimensional transient problems render these approaches computationally prohibitive. Another possibility is to assume that the pdf of a system state is either Gaussian or a given transform thereof, i.e., that it is fully described by its mean and variance [*Amir and Neuman*, 2001, 2004]. Even for relatively simple nonlinear problems (unsaturated flow described by Richards' equation), such Gaussian closure approaches proved to be limited to mildly heterogeneous formations [*Tartakovsky and Guadagnini*, 2001; *Tartakovsky et al.*, 2003]. Applications of

[1]Department of Mechanical and Aerospace Engineering, University of California, San Diego, La Jolla, California, USA.
[2]Department of Geotechnical Engineering and Geosciences, Technical University of Catalonia, Barcelona, Spain.
[3]Earth and Environmental Science Division, Los Alamos National Laboratory, Los Alamos, New Mexico, USA.

0043-1397/09/2008WR007383$09.00

the assumed pdf method [*Girimaji*, 1991] to solute transport in heterogeneous subsurface environments can be found in the work by, e.g., *Caroni and Fiorotto* [2005] and *Bellin and Tonina* [2007]. Assessment of the accuracy and robustness of such methods requires one to solve stochastic transport equations by Monte Carlo simulations or other means.

[5] The pdf methods provide an attractive alternative to these approaches by deriving a deterministic equation for the pdf of a system variable. In subsurface hydrology, equations for the pdf of the concentration of a conservative solute advected by a random velocity field were derived by *Indelman and Shvidler* [1985] and *Shvidler and Karasaki* [2003]. *Lichtner and Tartakovsky* [2003] obtained a pdf equation for a batch system undergoing kinetic reactions. An additional benefit of pdf methods is that they enable one to avoid a linearization of reactive transport equations. This nonlinearity arises through, for example, kinetic rate laws describing precipitation/dissolution of solids and kinetic sorption/desorption rates, as well as through incorporation of local equilibrium relations derived from the law of mass action for homogeneous and heterogeneous reactions. Moment equation approaches [e.g., *Espinoza and Valocchi*, 1997; *Reichle et al.*, 1998; *Dagan and Indelman*, 1999; *Miralles-Wilhelm and Gelhar*, 2000] generally require expanding the nonlinear terms about the local mean concentration of the system and retaining only linear terms. As a consequence, such approaches apply at best to small deviations from the mean, an approach that is inadequate for most natural geochemical systems [*Cirpka et al.*, 2008].

[6] A major goal of this study is to present a pdf formulation applied to advective transport of a contaminant that undergoes a heterogeneous chemical reaction involving an aqueous solution reacting with a solid phase. Section 2 contains a mathematical formulation of the problem. In section 3, we present closed form analytical solutions for the pdf of concentration for several statistical models of the kinetic rate constant. These are used to derive an effective transport equation and an effective kinetic rate constant in section 4.

2. Problem Formulation

[7] Consider a heterogeneous chemical reaction taking place in a porous medium between a dissolved species $\mathcal{C}$ and a solid $\mathcal{C}_{(s)}$,

$$\alpha\mathcal{C} \rightleftharpoons \mathcal{C}_{(s)}, \tag{1}$$

where α is the stoichiometric coefficient. The speed with which c, the concentration of $\mathcal{C}$, reaches its equilibrium level c_{eq} is determined from the product of the laboratory measured kinetic rate constant k_0 [mol L^{-2} T^{-1}] for reaction (1) and specific surface area A [L^{-1}] of a porous matrix, designated as k and referred to as the kinetic rate constant in what follows:

$$k = k_0 A c_{\mathrm{eq}}^{-\alpha}. \tag{2}$$

In this definition, the kinetic rate constant k [$(\mathrm{mol\,L}^{-3})^{1-\alpha}\,\mathrm{T}^{-1}$] includes the contribution from the specific surface area A, assumed to be constant in time in the following. On the local scale ω, the evolution of the solute concentration $c(\mathbf{x}, t)$ in steady macroscopic velocity field $\mathbf{v}(\mathbf{x}) = \mathbf{q}(\mathbf{x})/\phi$, where $\mathbf{q}(\mathbf{x})$ denotes Darcy's flux and ϕ is porosity, can be described by an advection-reaction equation (ARE)

$$\frac{\partial c}{\partial t} + \nabla \cdot (\mathbf{v}c) = -\frac{k}{\phi} f_\alpha(c), \qquad f_\alpha(c) \equiv \alpha\left(c^\alpha - c_{\mathrm{eq}}^\alpha\right), \tag{3}$$

where $f_\alpha(c)$ represents the product of the stoichiometric coefficient and the affinity factor giving the degree of disequilibrium. The transport equation is subject to the initial condition

$$c(\mathbf{x}, t = 0) = c_{\mathrm{in}}(\mathbf{x}) \tag{4}$$

and appropriate boundary conditions. The initial concentration c_{in} may be larger or smaller than the equilibrium concentration c_{eq} resulting in precipitation of the reacting species or dissolution of the solid matrix, respectively. It is worthwhile emphasizing that the methodology developed below is equally applicable to other types of chemical reactions and other functional forms of $f_\alpha(c)$.

[8] The transport model, (3) and (4) contains a number of implicit assumptions. First, following *Neuman* [1993], *Shvidler and Karasaki* [2003] and many others, we neglect dispersion on the local scale ω. In this view, dispersion is an emerging transport phenomenon that arises from velocity fluctuations and manifests itself on scales larger than ω. This is a reasonable assumption for transport phenomena in which mixing in the aqueous phase does not control reactions. Second, (3) breaks down when the reaction rate becomes large enough to produce gradients on the scale of the separation between solid grains. In such cases it is necessary to explicitly account for diffusion-controlled reaction at the surface of solid grains [e.g., *Tartakovsky et al.*, 2008]. Third, $k(\mathbf{x})$ is assumed to be independent of time. For the case of dissolution, as reaction proceeds the surface may in fact increase with time because of the formation of etch pits on the mineral surface. As individual grains completely dissolve the associated surface area would tend to zero. For the system considered here, it is assumed that equilibrium is reached before appreciable changes in grain surface can occur. For the case of precipitation it is assumed that the precipitating solid nucleates on the existing mineral surface although this need not necessarily be the case in general. Surface armoring effects, not considered here, could also result in a time-dependent surface area.

[9] A typical porous matrix exhibits highly nonuniform geometry, even if it is macroscopically homogeneous, i.e., even if its macroscopic hydraulic properties are constant. This is because natural porous media composed of an aggregate of mineral grains involve a distribution of grain sizes, typically over a wide range of values [*Clausnitzer and Hopmans*, 1999; *Tuli et al.*, 2001]. Since the kinetic rate constant $k(\mathbf{x})$ is determined by the reacting surface area (see its definition above), it cannot be determined with certainty on a typical local scale ω, let alone large scales used in predictive models of reactive transport. This lack of certainty can be quantified by treating $k(\mathbf{x})$ as a random field with the multivariate probability density function $\mathcal{P}[k(\mathbf{x})]$, from which one can compute its ensemble mean $\overline{k}$, variance σ_k^2, and two-point correlation function $\rho_k(\mathbf{x}, \mathbf{x}')$ with correlation length l.

[10] It is important to recognize that randomness in hydrogeology is a mathematical representation of uncertainty about our knowledge of the hydraulic and transport properties of the subsurface. In this study, we treat the kinetic reaction rate constant $k(\mathbf{x})$ as the sole source of uncertainty by regarding the remaining parameters in the reactive transport equation (3), e.g., the macroscopic flow velocity $\mathbf{v}(\mathbf{x})$, as deterministic. (The deterministic treatment of velocity $\mathbf{v}(\mathbf{x})$ implies that correlation length l_k of the random field $k(\mathbf{x})$ is larger than the characteristic length of the support volume ω, but much smaller than the variation scale of $\mathbf{v}$.) Likewise, the equilibrium concentration c_{eq} is assumed to be deterministic, as inferred from thermodynamic considerations. As discussed below, uncertainty in the initial concentration can be easily accounted for, even though we take c_{in} to be deterministic in order to simplify the presentation. Uncertainty (randomness) in flow velocity $\mathbf{v}(\mathbf{x})$ will be tackled in a follow up study.

[11] To be specific, we assume that the kinetic reaction rate constant $k(\mathbf{x})$ is a statistically homogeneous (stationary) random field, so that both $\overline{k}$ and σ_k^2 are constant and $\rho_k(\mathbf{x}, \mathbf{x}') \equiv \rho_k(|\mathbf{x} - \mathbf{x}'|)$. We use the Reynolds decomposition to represent the random field $k(\mathbf{x})$ as the sum of its ensemble mean $\overline{k}$ and zero-mean normalized fluctuations $k'(\mathbf{x})$,

$$k(\mathbf{x}) = \overline{k}[1 + k'(\mathbf{x})], \qquad \overline{k'(\mathbf{x})} = 0. \tag{5}$$

The two-point covariance function of the normalized fluctuations $k'(\mathbf{x})$ is given by

$$\overline{k'(\mathbf{x})k'(\mathbf{x}')} = \hat{\sigma}_k^2 \rho_k(\mathbf{x} - \mathbf{x}'), \qquad \sigma_k = \overline{k}\hat{\sigma}_k. \tag{6}$$

[12] Let us introduce dimensionless parameters and variables

$$\hat{\mathbf{x}} \equiv \frac{\mathbf{x}}{l}, \quad \hat{t} \equiv \frac{t}{\tau_q}, \quad \hat{k} \equiv \frac{k}{\overline{k}}, \quad \hat{\mathbf{v}} \equiv \frac{\mathbf{v}}{U}, \quad \hat{c} \equiv \frac{c}{c_{\mathrm{eq}}}, \tag{7}$$

where $\tau_q = l/U$ is the advection time scale that defines the time it takes solute transported by advection with characteristic (e.g., average) velocity U to travel one correlation length l. It follows from (7) that the dimensionless correlation scale is $\hat{l} = 1$. The dimensionless form of ARE (3) is given by

$$\frac{\partial \hat{c}}{\partial \hat{t}} + \hat{\nabla} \cdot (\hat{\mathbf{v}}\hat{c}) = -Da\, \hat{k} \hat{f}_\alpha(\hat{c}), \qquad \hat{f}_\alpha(\hat{c}) = \alpha(\hat{c}^\alpha - 1). \tag{8}$$

The Damköhler number $Da \equiv \tau_q\, \overline{k}\, c_{\mathrm{eq}}^{\alpha-1}/\phi$ compares the advection time scale τ_q with the reaction time scale $1/\overline{k}$. The dimensionless reaction time scale equals Da^{-1}. Equation (8) is subject to the initial condition $\hat{c}(\hat{\mathbf{x}}, 0) = \hat{c}_{\mathrm{in}}(\hat{\mathbf{x}})$, where $\hat{c}_{\mathrm{in}} \equiv c_{\mathrm{in}}/c_{\mathrm{eq}}$. In the following we drop the hats $\hat{}$ to simplify the notation.

3. The pdf Solutions

[13] Since the kinetic rate constant $k(\mathbf{x})$ is modeled as a random space function, the concentration distribution $c(\mathbf{x}, t)$ is a random function as well. Our goal is to determine the single-point distribution density of $c(\mathbf{x}, t)$, i.e., the distribution of concentration values at a point $(\mathbf{x}, t)$, which is defined by $p(c; \mathbf{x}, t) = \overline{\delta[c - c(\mathbf{x}, t)]}$. In the following, we derive an exact map between the pdf of the kinetic rate constant $k(\mathbf{x})$ and the concentration pdf $p(c; \mathbf{x}, t)$.

[14] Since $\nabla \cdot \mathbf{v} = 0$, a family of characteristics for (8) is given by

$$\frac{\mathrm{d}x_i}{\mathrm{d}t} = v_i(\mathbf{x}), \quad x_i(0) = \xi_i, \quad i = 1, 2, 3, \tag{9}$$

where x_i, v_i and ξ_i are the components of vectors $\mathbf{x}$, $\mathbf{v}$ and $\boldsymbol{\xi}$, respectively. Along the characteristics $\mathbf{x}(t)$, a solution of (8) takes the form $c[\mathbf{x}(t), t]$ and satisfies

$$\frac{\mathrm{d}c}{\mathrm{d}t} = -Da\, k[\mathbf{x}(t)] f_\alpha(c), \qquad f_\alpha(c) = \alpha(c^\alpha - 1) \tag{10}$$

subject to the initial condition $c(\mathbf{x}, 0) = c_{\mathrm{in}}(\boldsymbol{\xi})$. A solution of (10) is given implicitly by

$$\mathcal{F}_\alpha(c) = -Da\, \mathcal{K}(t), \qquad \mathcal{K}(t) \equiv \int_0^t k[\mathbf{x}(t')]\mathrm{d}t', \tag{11a}$$

where

$$\mathcal{F}_\alpha(c) \equiv \frac{c}{\alpha} {}_2F_1\left[\frac{1}{\alpha}, 1, 1 + \frac{1}{\alpha}, c^\alpha\right] - \frac{c_{\mathrm{in}}(\boldsymbol{\xi})}{\alpha} {}_2F_1\left[\frac{1}{\alpha}, 1, 1 + \frac{1}{\alpha}, c_{\mathrm{in}}^\alpha\right] \tag{11b}$$

and ${}_2F_1(a, b, c, x)$ is the hypergeometric function.

[15] For a given (deterministic) velocity field $\mathbf{v}(\mathbf{x})$, the characteristics $\mathbf{x}(t)$ can be obtained from (9). This, in turn, enables one to generate the random function $\mathcal{K}(t)$ in (11a). Given the implicit relation (11a) between concentration c and $\mathcal{K}$, $p(c; \mathbf{x}, t)$ can now be expressed in terms of $p_{\mathcal{K}}(K, t)$ as

$$p(c; \mathbf{x}, t) = \frac{1}{Da f_\alpha(c)} p_{\mathcal{K}}\left[-\frac{1}{Da}\mathcal{F}_\alpha(c), t\right]. \tag{12}$$

It remains to compute the pdf of $\mathcal{K}(t)$ in (12) in terms of the pdf of the kinetic reaction rate constant $k(t)$.

[16] To simplify the subsequent analysis, we take the flow velocity $\mathbf{v}$ to be constant and aligned with the x_1 coordinate, $\mathbf{v} = (U, 0, 0)^T$ or in dimensionless form $\hat{\mathbf{v}} = (1, 0, 0)^T$. It follows from (10) that $\mathbf{x}(t) = (x_1 - t, x_2, x_3)^T$. The statistical homogeneity (stationarity) of the random field $k(\mathbf{x})$ implies that for a fixed $\mathbf{x}$, the random field $k(x_1 - t, x_2, x_3)$ in (11a) is statistically equivalent to $k(t) \equiv k(t, 0, 0)$. The two-point correlation function of the fluctuations $k'(t) \equiv k'(t, 0, 0)$ is obtained from (6) as

$$\overline{k'(t)k'(t')} = \sigma_k^2 \rho_k(t - t', 0, 0). \tag{13}$$

(Note that the dimensional correlation time is τ_q, and its nondimensional counterpart is 1.) Thus, in the ensemble sense (11a) is equivalent to

$$\mathcal{F}_\alpha(c) = -Da\, \mathcal{K}(t), \qquad \mathcal{K}(t) = \int_0^t k(t')\mathrm{d}t'. \tag{14}$$

It follows from (14) that the mean and variance of $\mathcal{K}(t)$ are given by

$$\overline{\mathcal{K}(t)} = t \tag{15a}$$

and

$$\sigma^2_{\mathcal{K}}(t) = \sigma^2_k \int_0^t \int_0^t \rho_k(t' - t'')\mathrm{d}t'\mathrm{d}t'' = 2\sigma^2_k \int_0^t (t - s)\rho_k(s)\mathrm{d}s, \tag{15b}$$

respectively. The remainder of this section is devoted to the derivation of the full pdf of $\mathcal{K}(t)$ and thus the pdf of $c(\mathbf{x}, t)$.

3.1. Relaxation to Equilibrium

[17] We study here the nonequilibrium behavior of reactive transport and the relaxation to equilibrium. To this end, we focus on the regimes characterized by $Da \ll 1$, so that the correlation time of $k(t)$ is small relative to the reaction time scale. In other words, we derive the concentration pdf in (14) for the dimensionless time $1 \ll t < T$, where T is given in multiples of Da^{-1}. In this regime, the kinetic rate constant $k'(t)$ can be approximated by a (non-Gaussian) zero mean white noise,

$$\overline{k'(t)k'(t')} = \sigma^2_k \delta(t - t'), \tag{16}$$

where $\delta(\cdot)$ is the Dirac delta function. A single-variable pdf $p_k(k)$ completely characterizes $k(t)$. The white noise approximation (16) of the correlated process (13) is valid after a solute species travels many pore lengths.

[18] To be specific, we take the kinetic reaction rate $k(x)$ to be lognormal [e.g., *Lichtner and Tartakovsky*, 2003],

$$p_k(k) = \frac{1}{k\sqrt{2\pi\sigma^2}} \exp\left[-\frac{(\ln k + \sigma^2/2)^2}{2\sigma^2}\right], \tag{17}$$

so that $\overline{k} = 1$ and $\sigma^2_k = \mathrm{e}^{\sigma^2} - 1$, where σ^2 is the variance of $\ln k$. In sections 3.1.1 and 3.1.2, we present two alternative approaches for computing the pdf of $\mathcal{K}(t)$, i.e., for evaluating the stochastic integral in (14).

3.1.1. Random Walk Particle Tracking

[19] It follows from (14) that $\mathcal{K}(t)$ satisfies the linear Langevin equation

$$\frac{\mathrm{d}\mathcal{K}(t)}{\mathrm{d}t} = k(t), \qquad \mathcal{K}(0) = 0. \tag{18}$$

Its discretized form reads

$$\mathcal{K}^{(n+1)} = \mathcal{K}^{(n)} + k^{(n)}, \tag{19}$$

where $\Delta t = 1$; that is, time is measured in pore lengths traveled (recall that the time unit is defined by the time it takes the solute to traverse one correlation scale l). The white noise process $\{k^{(i)}\}_{i=1}^n$ is distributed according to

$$\mathcal{P}_k\{k^{(i)}\} = \exp\left\{\sum_{i=1}^n \ln\left[p_k\left(k^{(i)}\right)\right]\right\}. \tag{20}$$

[20] The concentration $c^{(n)}$ at the nth time step can now be obtained from the first equation in (14). This procedure is equivalent to solving the (nonlinear) Langevin equation,

$$\frac{\mathrm{d}c}{\mathrm{d}t} = -Da\, k(t) f_\alpha(c), \qquad c(\mathbf{x}, t = 0) = c_{\mathrm{in}}(\mathbf{x}), \tag{21}$$

using the Stratonovich interpretation [e.g., *Risken*, 1996]. The numerical random walk simulations presented in section 3.2 use 10^5 particles.

3.1.2. Gaussian Approximation

[21] According to the central limit theorem (CLT), the sum of ± independent identically distributed random variables whose mean is zero and whose variance σ^2_k is finite, is Gaussian with zero mean and variance $\sigma^2_k\, t$. This implies that the distribution of $\mathcal{K}(t)$ is approximately Gaussian,

$$p_{\mathcal{K}}(\mathcal{K}, t) \approx \frac{1}{\sqrt{2\pi\sigma^2_k t}} \exp\left[-\frac{(\mathcal{K} - t)^2}{2\sigma^2_k t}\right], \tag{22}$$

provided the dimensionless time t is large enough; that is, the solute has traveled over many pore lengths.

[22] For the lognormal distribution (17), the quality of this approximation depends strongly on σ^2, the variance of $\ln k$. Figure 1 compares the distribution of $\mathcal{K}(t)$ computed by solving the discretized Langevin equation (19) with its Gaussian counterpart, (22), for $\sigma = 1$ ($\sigma_k \approx 1.31$) and $\sigma = 2$ ($\sigma_k \approx 7.32$). After the solute travels approximately 10^3 pore lengths, a Gaussian form is achieved for $\sigma = 1$ but not for $\sigma = 2$.

[23] As outlined above, we investigate the nonequilibrium reactive transport regime and the relaxation to equilibrium. In this regime the solute can travel a large number of pore lengths, expressed as a multiple of Da^{-1}. Recall that Da^{-1} is equal to the dimensionless reaction time scale and thus measures the number of pore length traveled before the system crosses over to equilibrium on the reaction time scale. In this early preasymptotic time regime, the Gaussian approximation (22) is satisfactory if (1) Da is small enough (dimensionless time is large enough) to ensure that the solute samples a sufficiently large number of pore lengths and (2) the variance of $\ln k$ is not too large.

3.2. Computational Examples

[24] In this section we present simulation results for the dimensionless reaction term $f_\alpha(c) = \alpha\,(c^\alpha - 1)$ in which the stoichiometric coefficient is set to either $\alpha = 1$ or $\alpha = 2$. To be specific, we assume that the initial concentration is smaller than or equal to the equilibrium concentration, $c_{\mathrm{in}}(\mathbf{x}) \le 1$. This model describes dissolution of the solid $\mathcal{C}_{(s)}$ and results in a reactive system with the dimensionless concentration $c \in [0, 1]$. (The opposite process of precipitation can be handled as well by taking the initial concentration to be larger than the equilibrium concentration, resulting in $c_{\mathrm{in}}(\mathbf{x}) \ge 1$.)

[25] It follows from (11b) that

$$\mathcal{F}_\alpha(c) = \begin{cases} \ln(1 - c) - \ln[1 - c_{\mathrm{in}}(x_1 - t, \mathbf{y})] & \alpha = 1 \\ \operatorname{artanh}[c_{\mathrm{in}}(x_1 - t, \mathbf{y})] - \operatorname{artanh}(c) & \alpha = 2, \end{cases} \tag{23}$$

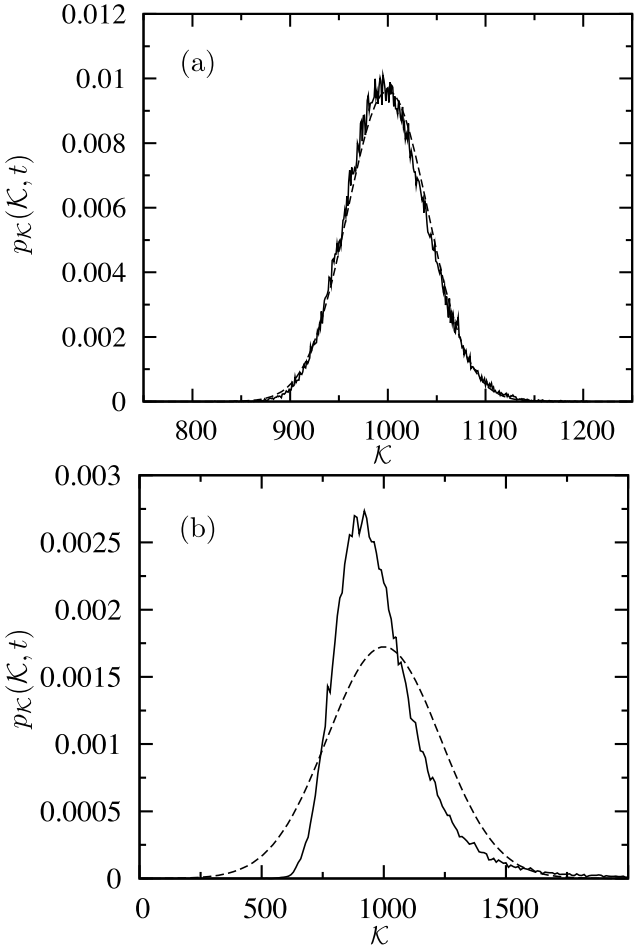

Figure 1. A snapshot at $t = 10^3$ of the pdf of $\mathcal{K}(t)$ for a lognormally distributed $k(t)$ with (a) $\sigma = 1$ and (b) $\sigma = 2$. The solid and dashed lines correspond to numerical simulations and the Gaussian approximation, respectively.

where $\mathbf{y} = (x_2, x_3)^T$. Combining the Gaussian approximation (22) with (23) and (12) we obtain analytical expressions for the pdf of concentration,

$$p(c;\mathbf{x},t) = \frac{1}{Da\sqrt{2\pi\sigma_k^2 t}} \begin{cases} \frac{1}{1-c}\mathrm{e}^{-\gamma_1(c,\mathbf{x},t)} & \alpha = 1 \\ \frac{1}{2(1-c^2)}\mathrm{e}^{-\gamma_2(c,\mathbf{x},t)} & \alpha = 2, \end{cases} \tag{24a}$$

where

$$\gamma_1(c,\mathbf{x},t) = \frac{1}{2\sigma_k^2 t}\left[Da^{-1}\mathcal{F}_1(c,\mathbf{x},t) + t\right]^2 \tag{24b}$$

$$\gamma_2(c,\mathbf{x},t) = \frac{1}{8\sigma_k^2 t}\left[Da^{-1}\mathcal{F}_2(c,\mathbf{x},t) + 2t\right]^2. \tag{24c}$$

[26] Figure 2 shows the temporal evolution of the pdf of concentration $p(c;\ \mathbf{x},\ t)$ for the nonlinear reaction with stoichiometric coefficient $\alpha = 2$ and lognormal kinetic reaction rate $k(\mathbf{x})$. For illustration, we present the results for a one-dimensional scenario in which $p(c;\ \mathbf{x},\ t)$ is independent of both x_2 and x_3. The Damköhler number is set to $Da = 10^{-3}$. Random walk simulations (solid lines) and the Gaussian approximation (dashed lines) are used to evaluate the pdf's at fixed $(x_1 - t) = 0$ for several values of t. The initial concentration at $x_1 = 0$ is given by $c_{\mathrm{in}}(0) = 0$. The Gaussian approximation (24a) performs well for $\sigma = 1$ (Figure 2a), but breaks down for $\sigma = 2$ for times shown in Figure 2b. This should come as no surprise, since the quality of the Gaussian approximation depends on the number of pore length traveled and thus on the time that has passed. It also depends on the variance σ^2 of ln k.

[27] As the system is driven toward its equilibrium concentration with increasing time, the region of highest probability moves along the c axis. The distribution is sharp at concentration values on the order of the initial concentration, and becomes more diffuse with increasing time up to $t \approx 250$. Then the distribution sharpens again as concentration moves further toward the equilibrium value of $c = 1$. In the asymptotic long time limit ($t \gg Da^{-1}$) the system approaches equilibrium; the pdf $p(c;\ \mathbf{x},\ t)$ becomes independent of space and time and is given by the delta distribution $p(c;\ \mathbf{x},\ t) = \delta(c - 1)$.

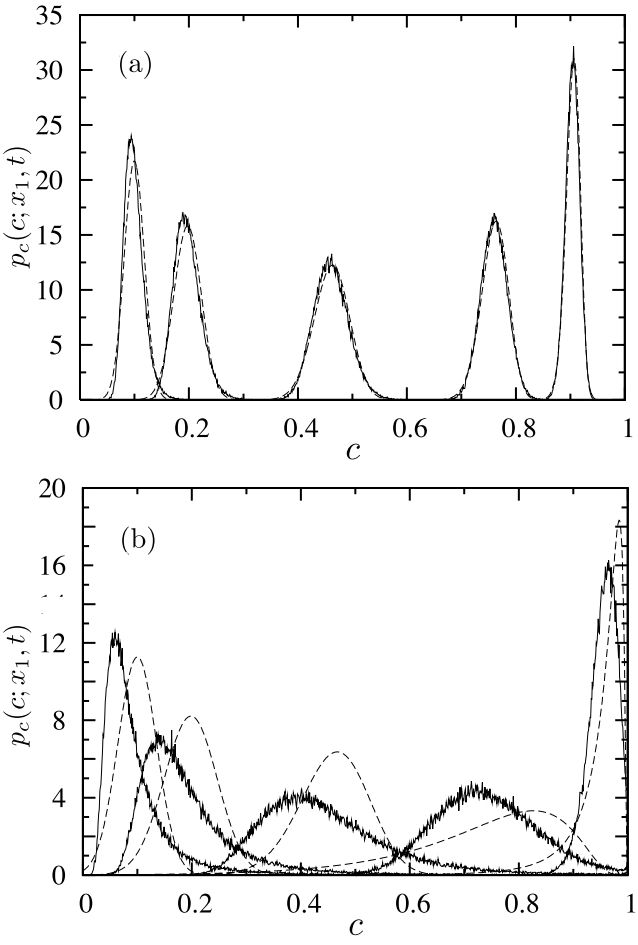

Figure 2. Snapshots of temporal evolution of the pdf of concentration $p(c;\ x_1,\ t)$ for (a) $\sigma = 1$ at times $t = 50$, 100, 250, 500, and 750 (from left to right) and (b) $\sigma = 2$ at times $t = 50$, 100, 250, 500, and 1000. The pdf is evaluated at constant $\xi = x_1 - t = 0$ using random walk simulations (solid lines) and the Gaussian approximation (dashed lines). The initial concentration at $x_1 = 0$ is $c_{\mathrm{in}}(0) = 0$.

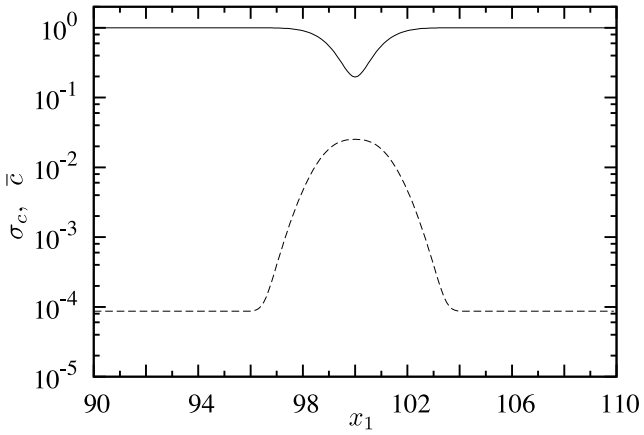

Figure 3. A snapshot (at $t = 100$) of average concentration $\bar{c}(x_1, t)$ (solid line) and standard deviation $\sigma_c(x_1, t)$ (dashed line) for nonlinear reactive transport with $\alpha = 2$ and $\sigma = 1$.

[28] As expected, the concentration pdf is sharper for $\sigma = 1$ (Figure 2a) than for $\sigma = 2$ (Figure 2b), reflecting an obvious fact that larger uncertainty in the input parameter k leads to larger predictive uncertainty. For $\sigma = 2$, the distribution of rate coefficients is much broader than for $\sigma = 1$ and the probability of encountering large rate coefficients is increased. The pdf $p(c; \mathbf{x}, t)$ spreads toward higher concentration values because at a given position the probability of being closer to equilibrium increases as the probability of encountering a fast kinetic rate constant increases.

4. Effective Transport Equations

[29] In subsurface hydrology, one is often interested in the mean behavior of a system, i.e., in the ensemble mean concentration $\bar{c}(\mathbf{x}, t)$. The latter can be computed by integrating the pdf of concentration

$$\bar{c}(\mathbf{x}, t) = \int_0^1 c p(c; \mathbf{x}, t) \mathrm{d}c, \tag{25}$$

or, equivalently, by solving a so-called effective transport equation. We obtain this equation below starting with the derivation of a deterministic equation that governs the evolution of the pdf $p(c; \mathbf{x}, t)$.

4.1. The pdf Equation

[30] When the kinetic rate constant $k(\mathbf{x})$ can be approximated by a Gaussian white noise (see the discussion in section 3.1), the Langevin equation (21) gives rise to the Fokker-Planck equation for the pdf $p(c; \mathbf{x}, t)$ (in the Stratonovich interpretation) [e.g., *Risken*, 1996],

$$\frac{\mathrm{d}p}{\mathrm{d}t} = \frac{\partial}{\partial c}\left[\left(Da - \frac{\sigma_k^2 Da^2}{2}\frac{\mathrm{d}f_\alpha}{\mathrm{d}c}\right) f_\alpha p\right] + \frac{\sigma_k^2 Da^2}{2}\frac{\partial^2 f_\alpha^2 p}{\partial c^2}. \tag{26}$$

We use here the Stratonovich interpretation because it honors the fact that $k(\mathbf{x})$ is correlated on the small scale. The initial condition for $p(c; \mathbf{x}, t)$ is given by the pdf for the initial concentration $c_{\mathrm{in}}(\mathbf{x})$. If the initial concentration is known with certainty, i.e., deterministic, then $p(c; \mathbf{x}, 0) = \delta[c - c_{\mathrm{in}}(\mathbf{x})]$.

[31] The boundary conditions for $p(c; \mathbf{x}, t)$ at $c = 0$ and $c = 1$ are specified in a manner that conserves the probability, i.e., satisfies the condition

$$\int_0^1 p(c; \mathbf{x}, t) \mathrm{d}c = 1. \tag{27}$$

[32] A few general comments are in order. First, one can verify by substitution that the pdf's $p(c; \mathbf{x}, t)$ given by either (14) and (22) or (24a) are indeed solutions of (26). Second, the limit of $\sigma_k^2 \to 0$ is a singular limit as it changes the order of the partial differential equation (26). Thus, solutions based on small perturbation expansions σ_k^2, a prevailing approach in stochastic hydrogeology, are not guaranteed to converge.

4.2. Effective Transport Equation

[33] We obtain an effective equation for the average concentration (25) by multiplying both sides of the pdf equation (26) with c and integrating over c from 0 to 1. After accounting for the boundary conditions for the pdf, this yields

$$\frac{\partial \bar{c}}{\partial t} + \frac{\partial \bar{c}}{\partial x} = -Da \int_0^1 \left[f_\alpha(c) - \frac{\sigma_k^2 Da}{4}\frac{\mathrm{d}f_\alpha^2}{\mathrm{d}c}\right] p(c; \mathbf{x}, t) \mathrm{d}c, \tag{28}$$

where boundary terms of the type $p(0, \mathbf{x}, t)$ are subleading for $Da \ll 1$ and are disregarded.

[34] For the dimensionless reactive term $f_\alpha(c) = \alpha(c^\alpha - 1)$ with the stoichiometric coefficient $\alpha = 1$, the effective transport equation (28) reduces to

$$\frac{\partial \bar{c}}{\partial t} + \frac{\partial \bar{c}}{\partial x} = -Da\left(1 - \frac{\sigma_k^2 Da}{2}\right)(\bar{c} - 1). \tag{29}$$

Its solution yields the mean concentration

$$\bar{c}(\mathbf{x}, t) = 1 - \exp\left(-Da\, t + \frac{\sigma_k^2 Da^2}{2} t\right)[1 - c_{\mathrm{in}}(x_1 - t, \mathbf{y})]. \tag{30}$$

It follows from (30) that perturbation expansions in σ_k^2 are bound to fail as time increases, even if $\sigma_k^2 \ll 1$.

[35] For $\alpha = 2$, the effective transport equation (28) becomes

$$\frac{\partial \bar{c}}{\partial t} + \frac{\partial \bar{c}}{\partial x} = -2Da\left(\overline{c^2} - 1\right) + 4\sigma_k^2 Da\left(\overline{c^3} - \bar{c}\right). \tag{31}$$

[36] Comparison of the effective equations (29) and (31) with their stochastic counterpart, (8), reveals that the two descriptions can be fundamentally different, so that effective parameters do not generally exist. The effective and stochastic descriptions have the same functional form only when the reaction term is linear ($\alpha = 1$).

[37] The computational examples presented in the following are one-dimensional and correspond to the deterministic initial concentration

$$c_{\mathrm{in}}(x_1) = 1 - \mathrm{e}^{-x_1^2/2}. \tag{32}$$

[38] Figure 3 presents the mean concentration $\bar{c}(x_1, t)$ given by the solution of the nonlinear ($\alpha = 2$) effective transport equation (31) at time $t = 100$. It is accompanied by

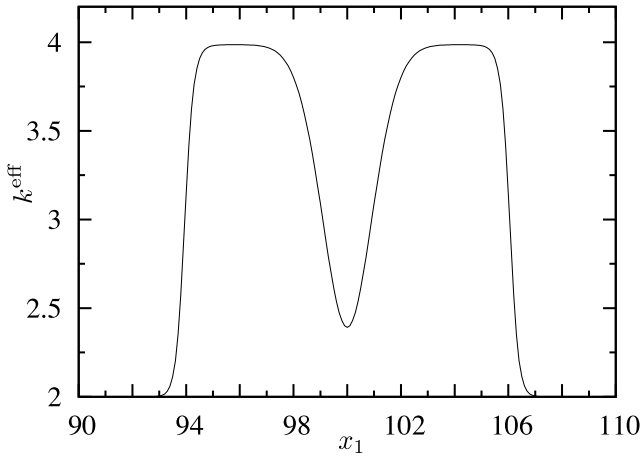

Figure 4. A snapshot ($t = 100$) of the effective kinetic rate constant $k^{\text{eff}}(x_1, t)$ for the nonlinear reaction with $\alpha = 2$ and $\sigma = 1$.

the standard deviation of concentration $\sigma_c(x_1, t)$, which was computed from the concentration variance

$$\sigma_c^2(x_1,t) = \int_0^1 [c - \overline{c}(x_1,t)]^2 p(c;x_1,t)\mathrm{d}c. \tag{33}$$

Both the best estimate of the concentration, $\overline{c}(x_1, t)$, and a measure of predictive uncertainty, $\sigma_c(x_1, t)$, are computed at the dimensionless time $t = 100$ for $\sigma^2 = 1$ and $Da = 10^{-3}$. At any given time, the mean concentration remains constant except for the regions where the traveling wave $c_{\text{in}}(x_1 - t)$ passes through. The center of this region, the point $x_1 = 100$ in the results reported in Figure 3, is the center of mass of the traveling wave. Uncertainty, as quantified by the standard deviation σ_c, remains unchanged in the region of constant mean concentration. Elsewhere, it increases as the mean concentration decreases. This is complementary to our observation in section 3.2, where we found that the pdf of concentration sharpens (i.e., variance is reduced) as the mean concentration increases.

[39] The temporal evolution of the mean concentration and standard deviation is analogous to the spatial behavior and is not displayed here.

4.3. Effective Transport Coefficients

[40] In section 4 we have shown that effective equations differ functionally from their local-scale counterparts, unless the reaction term is linear ($\alpha = 1$). Yet, the prevailing approach is to search for a standard, but not necessarily correct, apparent equation

$$\frac{\partial \overline{c}}{\partial t} + \frac{\partial \overline{c}}{\partial x_1} = -Da\, k^{\text{eff}}(\mathbf{x},t)[\overline{c}^{\alpha} - 1]. \tag{34}$$

Following the approach of *Lichtner and Tartakovsky* [2003], we derive such an equation by comparing (34) with (28). The requirement that the two be equivalent gives

$$k^{\text{eff}}(\mathbf{x},t) = \frac{1}{\overline{c}^{\alpha} - 1} \int_0^1 \left[1 - \sigma_k^2 Da \frac{\mathrm{d}f_{\alpha}}{\mathrm{d}c}\right] f_{\alpha}(c) p(c;\mathbf{x},t)\mathrm{d}c, \tag{35}$$

where we used the fact that $f_{\alpha}(c = 1) = 0$.

[41] For the linear reaction with the stoichiometric coefficient $\alpha = 1$, (35) gives

$$k^{\text{eff}} = 1 - \frac{\sigma_k^2 Da}{2}, \tag{36}$$

which can be verified by the direct comparison of (8) and (29). In this case, the effective and apparent equations coincide, and the effective kinetic reaction rate constant k^{eff} arises naturally.

[42] It is interesting to note that the effective kinetic rate constant k^{eff} for a reactive batch system (i.e., a system without advection) varies in time, tending to zero as time becomes large [*Lichtner and Tartakovsky*, 2003]. Here, the effective kinetic rate k^{eff} is constant and smaller than the mean reaction rate. This can be explained by the fact that a solute "samples" the chemical heterogeneity of a medium as it migrates along its flow pathway in a single realization. Only after the solute has sampled the heterogeneity over many correlation lengths does the local reaction rate law become valid on a large scale. For the batch system, a single medium realization is homogeneous and the concentration statistics reflect purely the differences between realizations. The effective rate tends to zero with time because the proper average over the reactive system approaches equilibrium faster than the mean reaction law that has the same appearance as the local reaction law.

[43] For $\alpha = 2$, the effective kinetic rate constant is given by

$$k^{\text{eff}}(\mathbf{x},t) = \frac{2}{\overline{c} - 1}\left[\overline{c^2} - 2\sigma_k^2 Da\left(\overline{c^3} - \overline{c}\right) - 1\right]. \tag{37}$$

The nth moment of concentration in (37) can be computed as

$$\overline{c(\mathbf{x},t)^n} = \int_{-\infty}^{\infty} p_{\mathcal{K}}(\mathcal{K},t) \times \left\{2\left[1 + \frac{1 - c_{\text{in}}(x_1 - t,\mathbf{y})}{1 + c_{\text{in}}(x_1 - t,\mathbf{y})}\mathrm{e}^{-4Da(\mathcal{K}+t)}\right]^{-1} - 1\right\}^n \mathrm{d}\mathcal{K}, \tag{38}$$

where $p_{\mathcal{K}}(\mathcal{K}, t)$ is given by its Gaussian approximation (22). Note that the effective kinetic rate for the nonlinear reaction is a function of space and time. The initial value of the effective kinetic rate constant can be evaluated explicitly,

$$k^{\text{eff}}(\mathbf{x},0) = 2\frac{c_{\text{in}}^2(\mathbf{x}) - 2\sigma_k^2 Da\left[c_{\text{in}}^3(\mathbf{x}) - c_{\text{in}}(\mathbf{x})\right] - 1}{c_{\text{in}}(\mathbf{x}) - 1}. \tag{39}$$

[44] The computational examples shown are one dimensional and correspond to the initial distribution (32). Figure 4 provides a snapshot of $k^{\text{eff}}(x_1, t = 100)$. The effective rate is constant far away from the bulk concentration, which is located at $x_1 = 100$. It increases in the vicinity of $x = 100$ where the mean concentration starts to change (see also Figure 3), reaches its maximum values closer to the center of mass of $\overline{c}(\mathbf{x}, t)$, and then decreases to a local minimum value at the center of mass. The increase of $k^{\text{eff}}(x_1, t)$ reflects the fact that the system is more reactive when the mean

concentration deviates from equilibrium. At the plateau value, the actual average reaction and the assumed mean reaction law as expressed by the definition (35) differ only by a constant factor. Closer to the center of mass of the mean reaction, however, the temporal change of the actual mean concentration is faster than the one predicted by the assumed mean reaction law (34).

5. Conclusions

[45] We presented an approach for computing pdf's of the concentration of a reactive solute that is being advected by a deterministic velocity field. Our analysis leads to the following major conclusions.

[46] 1. While many standard techniques for uncertainty quantification in groundwater hydrology yield only concentration's mean and variance, the proposed approach leads to its full probabilistic description. This allows one to compute so-called rare event (distribution tails), which are required in modern probabilistic risk analyses.

[47] 2. The shape and type of the pdf change in time. They vary between the known initial and steady state distributions that are given by the Dirac delta functions when both the initial and equilibrium concentrations are known with certainty. This makes reliance on a single assumed form of the pdf problematic.

[48] 3. Effective (averaged) transport equations are generally different from their local-scale (stochastic) counterparts.

[49] 4. Effective parameters for average reactive transport equations do not generally exist because of the nonlinearity of the latter. Effective parameters in apparent advection-reaction equations can vary in space and time.

[50] 5. Perturbation expansions routinely used to predict flow and transport in ''mildly heterogeneous'' porous media fail when applied to advection-reaction transport.

[51] While the presented methodology is applicable to any deterministic flow velocity fields $\mathbf{v}(\mathbf{x}, t)$ for which a solution of (9) exists, we considered the simplest case of constant velocity to simplify the presentation. In follow up studies, we will extend this analysis to the cases of space-time variable deterministic velocity fields and uncertain (random) velocity fields.

[52] **Acknowledgments.** We thank the two anonymous reviewers and the Associate Editor Olaf Cirpka for their invaluable comments. This research was partially supported by the DOE Office of Science Advanced Scientific Computing Research program in Applied Mathematical Sciences and by the Office of Science (BER), cooperative agreement DE-FC02-07ER64324. M.D. gratefully acknowledges the financial support of the program Ramón y Cajal of the Spanish Ministry of Science and Education and through a travel grant by the Catalan Agency for Administration of Universities and Research.

References

Amir, O., and S. P. Neuman (2001), Gaussian closure of one-dimensional unsaturated flow in randomly heterogeneous soils, *Transp. Porous Media*, *44*(2), 355–383.

Amir, O., and S. P. Neuman (2004), Gaussian closure of transient unsaturated flow in random soils, *Transp. Porous Media*, *54*(1), 55–77.

Bellin, A., and D. Tonina (2007), Probability density function of non-reactive solute concentration in heterogeneous porous formations, *J. Contam. Hydrol.*, *94*, 109–125.

Bellin, A., A. Rinaldo, W. J. P. Bosma, S. E. A. T. M. van der Zee, and Y. Rubin (1993), Linear equilibrium adsorbing solute transport in physically and chemically heterogeneous porous formations: 1. Analytical solutions, *Water Resour. Res.*, *29*(12), 4019–4030.

Caroni, E., and V. Fiorotto (2005), Analysis of concentration as sampled in natural aquifers, *Transp. Porous Media*, *59*(1), 19–45.

Cirpka, O. A., R. L. Schwede, J. Luo, and M. Dentz (2008), Concentration statistics for mixing-controlled reactive transport in random heterogeneous media, *J. Contam. Hydrol.*, *98*, 61–74.

Clausnitzer, V., and J. W. Hopmans (1999), Determination of phase-volume fractions from tomographic measurements in two-phase systems, *Adv. Water Resour.*, *22*, 577–584.

Dagan, G., and P. Indelman (1999), Reactive solute transport inflow between a recharging and a pumping well in a heterogeneous aquifer, *Water Resour. Res.*, *35*(12), 3639–3647.

Espinoza, C., and A. J. Valocchi (1997), Stochastic analysis of one-dimensional transport of kinetically adsorbing solutes in chemically heterogeneous aquifers, *Water Resour. Res.*, *33*(11), 2429–2445.

Girimaji, S. S. (1991), Assumed β-pdf model for turbulent mixing: Validation and extension to multiple scalar mixing, *Combust. Sci. Technol.*, *78*, 177–196.

Indelman, P. V., and M. I. Shvidler (1985), Averaging of stochastic evolution equations of transport in porous media, *Fluid Dyn.*, *20*(5), 775–784, Engl. Transl..

Lastoskie, C., K. E. Gubbins, and N. Quirke (1993), Pore size distribution analysis of microporous carbons: A density functional theory approach, *J. Phys. Chem.*, *97*(18), 4786–4796.

Lichtner, P. C., and D. M. Tartakovsky (2003), Stochastic analysis of effective rate constant for heterogeneous reactions, *Stochastic Environ. Res. Risk Assess.*, *17*(6), 419–429.

Miralles-Wilhelm, F., and L. W. Gelhar (2000), Stochastic analysis of oxygen-limited biodegradation in heterogeneous aquifers with transient microbial dynamics, *J. Contam. Hydrol.*, *42*, 69–97.

Neuman, S. P. (1993), Eulerian-Lagrangian theory of transport in space-time nonstationary velocity fields: Exact nonlocal formalism by conditional moments and weak approximation, *Water Resour. Res.*, *29*(3), 633–645.

Reichle, R., W. Kinzelbach, and H. Kinzelbach (1998), Effective parameters in heterogeneous and homogeneous transport models with kinetic sorption, *Water Resour. Res.*, *34*(4), 583–594.

Risken, H. (1996), *The Fokker-Planck Equation*, Springer, New York.

Rubin, Y. (2003), *Applied Stochastic Hydrogeology*, Oxford Univ. Press, New York.

Shvidler, M., and K. Karasaki (2003), Probability density functions for solute transport in random field, *Transp. Porous Media*, *50*(3), 243–266.

Srinivasan, G., D. M. Tartakovsky, B. A. Robinson, and A. B. Aceves (2007), Quantification of uncertainty in geochemical reactions, *Water Resour. Res.*, *43*, W12415, doi:10.1029/2007WR006003.

Tartakovsky, A. M., D. M. Tartakovsky, T. D. Scheibe, and P. Meakin (2008), Hybrid simulations of reaction-diffusion systems in porous media, *SIAM J. Sci. Comput.*, *30*(6), 2799–2816.

Tartakovsky, D. M. (2007), Probabilistic risk analysis in subsurface hydrology, *Geophys. Res. Lett.*, *34*, L05404, doi:10.1029/2007GL029245.

Tartakovsky, D. M., and A. Guadagnini (2001), Prior mapping for nonlinear flows in random environments, *Phys. Rev. E*, *64*, 035302, doi:10.1103/PhysRevE.64.035302.

Tartakovsky, D. M., A. Guadagnini, and M. Riva (2003), Stochastic averaging of nonlinear flows in heterogeneous porous media, *J. Fluid Mech.*, *492*, 47–62.

Tuli, A., K. Kosugi, and J. W. Hopmans (2001), Simultaneous scaling of soil water retention and unsaturated hydraulic conductivity functions assuming lognormal pore-size distribution, *Adv. Water Resour.*, *24*, 677–688.

Winter, C. L., and D. M. Tartakovsky (2008), A reduced complexity model for probabilistic risk assessment of groundwater contamination, *Water Resour. Res.*, *44*, W06501, doi:10.1029/2007WR006599.

M. Dentz, Department of Geotechnical Engineering and Geosciences, Technical University of Catalonia, E-08034 Barcelona, Spain. (marco.dentz@upc.edu)

P. C. Lichtner, Earth and Environmental Science Division, Los Alamos National Laboratory, Los Alamos, NM 87545, USA. (lichtner@lanl.gov)

D. M. Tartakovsky, Department of Mechanical and Aerospace Engineering, University of California, San Diego, 9500 Gilman Drive, Mail Code 0411, La Jolla, CA 92093, USA. (dmt@ucsd.edu)